

# Raman spectroscopy studies of the high-temperature evolution of the free carbon phase in polycarbosilane derived SiC ceramics

Ma Yan<sup>\*</sup>, Wang Song, Chen Zhao-hui

*Key Lab of Advanced Ceramic Fibers & Composites, College of Aerospace & Materials Engineering,  
National University of Defense Technology, Changsha 410073, PR China*

Received 6 April 2010; received in revised form 30 April 2010; accepted 4 July 2010

Available online 7 August 2010

## Abstract

The Raman spectra of a number of SiC ceramics synthesized from polycarbosilane at 1200 °C and annealed at 1400, 1600, 1800 and 2000 °C have been recorded using laser excitation wavelength of 532 nm. The peak positions, their intensities ( $I_D/I_G$ ) and full width at half maximum (FWHM) were used to obtain information about the degree of disorder in the free carbon phases. The increasing ordering with annealing temperature was confirmed by lower FWHM values and G-peak positions obtained from the SiC ceramics annealed at higher temperature. However, the  $I_D/I_G$  has shown to be the highest point at 1600 °C, which illustrates that the temperature is one critical point of the microstructure evolution of the free carbon phase changing amorphous to turbostratic with increasing temperatures. Obviously, the oxidation behaviors of the SiC ceramics are significantly affected by the microstructures of the free carbon phases. In the SiC ceramics with above 1600 °C annealing, the oxidation temperatures of the SiC phases are postponed more than 100 °C, because they are surrounded by the free carbon phases.

© 2010 Elsevier Ltd and Techna Group S.r.l. All rights reserved.

**Keywords:** Ceramics; Annealing; Raman spectroscopy; Microstructure

## 1. Introduction

Organosilicon polymers have been studied extensively since Yajima et al. [1] invented SiC fiber from polycarbosilane (PCS). Now, one kind of the most popular precursors is PCS [2,3] with ramifications, such as polyvinylsilane [4], polydimethylsilane [5], allylhydridopolycarbosilane [6].

The characteristics of SiC ceramics derived from these precursors are determined by the architectures of initial precursors, the mechanisms of thermal transformations between precursors and ceramic products, and the evolutions of ceramic products with high-temperature thermal treatment (above 1000 °C). As reported, the origin of the excess carbon is due to the crackings of intermediately formed aliphatic hydrocarbons and their reorganizations toward aromatic hydrocarbons whose pyrolysis yield the so-called free carbon at  $T_p \approx 600$  °C [7]. So the free carbon always is an important component in SiC ceramics derived from PCS. In the opinion of

Okamura et al. [8] and Laine et al. [9,10], the amorphous and graphite-like carbon plays a positive role in stabilizing the ceramic phase, because the carbon present at boundaries of SiC grains act as diffusion barriers preventing the grain growth and coalescence of the SiC microcrystal. However, the role of the free carbon in the SiC ceramics derived from precursors appears not to be singular, because the crystallization and distribution of the free carbon can be changed in the annealing conditions. So many properties of the SiC ceramics will be affected by the microstructures of the free carbon phases.

Raman spectroscopy is a standard non-destructive analysis tool for characterization of various carbon materials. Carbon materials typically exhibit two main bands, D (disordered) and G (graphitic) peak, usually assigned to zone center phonons of  $E_{2g}$  symmetry and K-point phonons of  $A_{1g}$  symmetry, respectively [11]. The unusual fact is that the presence and position of D and G peak, their intensities ( $I_D$  and  $I_G$ ) and full width at half maximum (FWHM) can be used to extract structural information of the materials.

Therefore, we present the Raman spectra of PCS derived SiC ceramics with various temperature thermal treatments, and the oxidation characteristics of the SiC ceramics are also compared.

<sup>\*</sup> Corresponding author. Tel.: +86 731 4576397; fax: +86 731 4573165.

E-mail address: [fogclock@sohu.com](mailto:fogclock@sohu.com) (M. Yan).

## 2. Experimental procedure

### 2.1. Substrate material

PCS with molecular weight  $\sim 1742$  and softening point  $\sim 175^\circ\text{C}$  was synthesized in our laboratory. It was pyrolyzed at  $1200^\circ\text{C}$  for 1 h (defined as raw sample), when the high purity  $\text{N}_2$  was used as the protective atmosphere. Then in Ar, the raw sample was separately treated at  $1400$ ,  $1600$ ,  $1800$  and  $2000^\circ\text{C}$  for 1 h. All experiments were carried out at a heating/cooling rate of  $500^\circ\text{C/h}$  to the desired temperature.

### 2.2. Analytical methods

Raman spectra were obtained using a SENTERRA spectrometer (Bruker) employing a semiconductor laser ( $\lambda = 532\text{ nm}$ ). Two types of decomposition were attempted by computer using Origin software developed by Microcal Software, which were based on three-band or four-band hypotheses. X-ray diffraction (XRD) measurements were performed using a Bruker diffractometer (Model D8 ADVANCED, Cu  $\text{K}\alpha$  radiation;  $\lambda = 1.5406\text{ \AA}$ ). Thermogravimetric analysis (TGA, NETZSCH STA 449C) was performed under an atmosphere of air, according to a heating/cooling rate of  $10^\circ\text{C/min}$ . The elementary analysis of the ceramic products was made on LECO CS600 for C and TCH600 for O and H, when the weight concentration of Si was confirmed by the perchloric acid dehydration-gravimetric method.

Transmission electron microscopic (TEM) analysis was performed by a JEOL JEM-2010 (Tokyo, Japan) operating at an acceleration voltage of  $200\text{ kV}$ .

## 3. Results and discussion

The compositions of the SiC ceramics before and after  $1800^\circ\text{C}$  annealing are shown in Table 1. In the raw sample, there are a considerable amount of elemental C (called as free carbon) and a little of elemental H. The residual H in the ceramic products is beneficial to prevent the crystallization of the free carbon early. After  $1800^\circ\text{C}$  annealing, the concentration of elemental O decreased, Si increased and C kept  $37\text{ wt.}\%$ . Indeed, a little of Si was also eliminated, because the weight loss ratio of the raw sample arrived at  $6.64\text{ wt.}\%$ . The reason of the weight loss is mainly the carbothermic reductions as following reactions (1) and (2) [3,12].

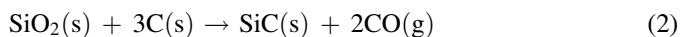
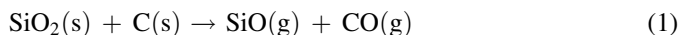


Table 1  
Chemical composition of the SiC ceramics before and after  $1800^\circ\text{C}$  annealing.

Sample	Composition (wt.%)				Stoichiometry	C/Si (at.%)
	Si	C	O	H		
Raw sample	58.37	37.05	1.99	0.19	$\text{SiC}_{0.99}\text{O}_{0.06}\text{H}_{0.09} + \text{C}_{0.48}$	1.47
Treated sample	60.03	37.02	0.56	–	$\text{SiC}_{0.99}\text{O}_{0.02} + \text{C}_{0.45}$	1.44

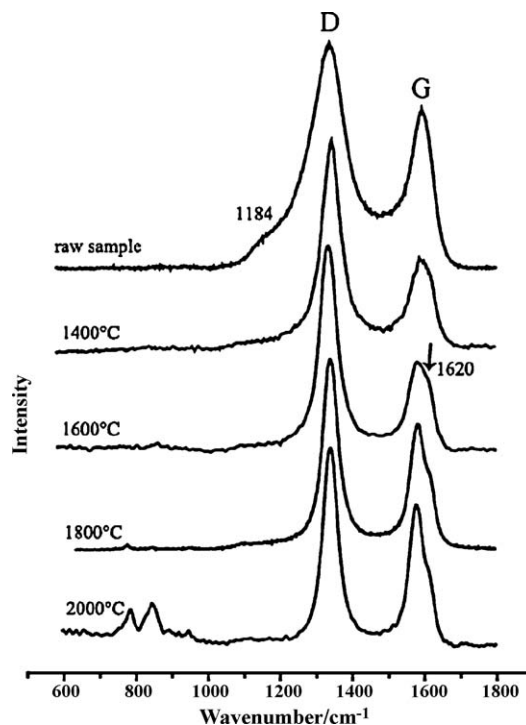


Fig. 1. Raman spectra of the SiC ceramics with various temperature thermal treatments.

Raman spectra of the SiC ceramics with various temperature thermal treatments are presented in Fig. 1, two main peaks and the Raman characteristics of the free carbon phases are shown in Table 2. Obviously, there were significant changes after annealing the SiC ceramics at high temperatures. The  $1184\text{ cm}^{-1}$  band disappeared, the  $1340$  and  $1600\text{ cm}^{-1}$  bands were narrowed and the  $1620\text{ cm}^{-1}$  band was present.

The  $1150$  and  $1480\text{ cm}^{-1}$  bands are thought as a signature of transpolyacetylene by Ferrari and Robertson [13], so they all disappeared after high-temperature thermal treatments. The FWHM of the G peak decreased from  $66.0$  to  $36.8\text{ cm}^{-1}$ , and the position shifted to *ca.*  $1580\text{ cm}^{-1}$  (in Table 2) with increasing temperatures, indicating that an ordering process occurred within the free carbon phases [14].

The intensity ratio  $I_D/I_G$  is related to the cluster diameter or in-plane correlation length,  $L_a$ , of the free carbon domains, as reported by Tuinstra and Koenig ( $I_D/I_G \propto L_a^{-1}$ ) for crystalline carbon [15] and recently by Ferrari and Robertson ( $I_D/I_G \propto L_a^2$ ) in the case of amorphous carbon [11,13]. Obviously,  $L_a$  became

Table 2  
Raman characteristics of the free carbon phases with various temperature thermal treatments.

Thermal temperature ( $^\circ\text{C}$ )	G peak		$I_D/I_G$
	Position ( $\text{cm}^{-1}$ )	FWHM ( $\text{cm}^{-1}$ )	
— <sup>a</sup>	1600	66.0	1.63
1400	1599	65.7	2.65
1600	1585	51.3	2.70
1800	1583	42.8	1.67
2000	1580	36.8	1.53

<sup>a</sup> The Raman characteristics of raw sample.

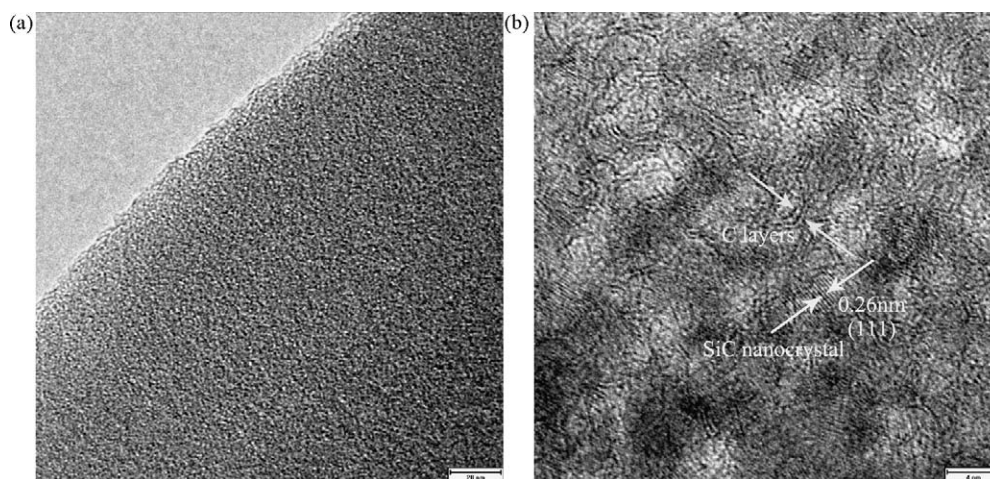


Fig. 2. The TEM images of the SiC ceramics (a) before and (b) after 1800 °C annealing.

larger with the higher annealing temperature. For the free carbon domains in the SiC ceramics, they were amorphous in the raw sample, and they had already been turbostratic after 1800 °C annealing (in Fig. 2). So  $I_D/I_G$  ratio increased at first up to 1600 °C, and then decreased with an increase of the annealing temperature. Consequently, for the free carbon phases in the SiC ceramics, the 1600 °C is the critical point of the microstructure evolution from amorphous carbon to graphite, and the  $1620\text{ cm}^{-1}$  shoulder characteristic of the imperfect graphite crystal [15,16] was well resolved (in Fig. 1), as a further proof.

The spectrum of the raw sample shows that the content of carbon species was lower than that given by the results of chemical analysis (in Table 1). This contraction was explained that the free carbon dissolved in the amorphous SiC continuum (with composition  $\text{Si}_{1-x}\text{C}_{1+x}$ ) did not contribute to the Raman spectra of carbon species [14,17].

However, when SiC spectral fingerprints are observed in Fig. 1, the annealing temperature was already 1800 °C, and the SiC nanocrystals were present well (in Fig. 2(b)). The reason is that the Raman scattering efficiency of carbon species can be assumed to be at least ten times higher than that of pure SiC materials, owing to their optical absorption [14].

As seen in Fig. 2, the SiC ceramics became nanocrystalline from amorphous after 1800 °C annealing, and the SiC nanocrystals (about 7 nm) were surrounded by the turbostratic carbon [18,19].

Fig. 3 shows the SiC Raman fingerprints of the SiC ceramics after 1800 and 2000 °C annealing. For 3C-SiC (known as  $\beta$ -SiC), which is the most frequently observed type below 2000 °C (in Fig. 3(a)), the energies of zone-centre transverse optical (TO) and longitudinal optical (LO) phonon have been reported to be at  $796$  and  $973\text{ cm}^{-1}$ . And the 6H-SiC (a kind of  $\alpha$ -SiC) spectrum shows a weak peak in the TO region at the same position as 3C ( $796\text{ cm}^{-1}$ ), the strongest peak is located at  $789\text{ cm}^{-1}$  while the peak position in the LO region is  $967\text{ cm}^{-1}$  [14], seen in Fig. 3(b). According to the concept of ‘large zone and zone folding’ [20], satellite lines appeared in the polytype spectra, shown about  $760\text{ cm}^{-1}$  in Fig. 3. They illuminated two kinds of SiC ( $\beta$ -SiC and  $\alpha$ -SiC) present in the SiC ceramics.

And the microstructure evolutions of the SiC phases are also confirmed by XRD (in Fig. 4). In Fig. 4, the raw sample is amorphous, but the crystallizations of the SiC phases evidently increased as the  $\beta$ -SiC after 1600 °C annealing, identified by the peaks at  $35.65^\circ$  ( $d = 2.516\text{ \AA}$ ),  $41.40^\circ$  ( $d = 2.179\text{ \AA}$ ),  $60^\circ$  ( $d = 1.540\text{ \AA}$ ) and  $71.78^\circ$  ( $d = 1.314\text{ \AA}$ ). When the SiC

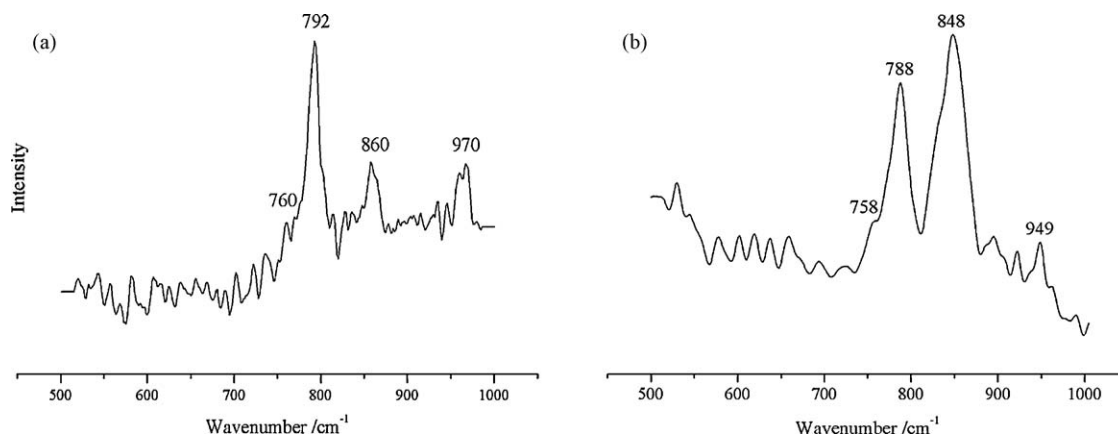


Fig. 3. SiC Raman fingerprints of the SiC ceramics after (a) 1800 °C and (b) 2000 °C annealing.

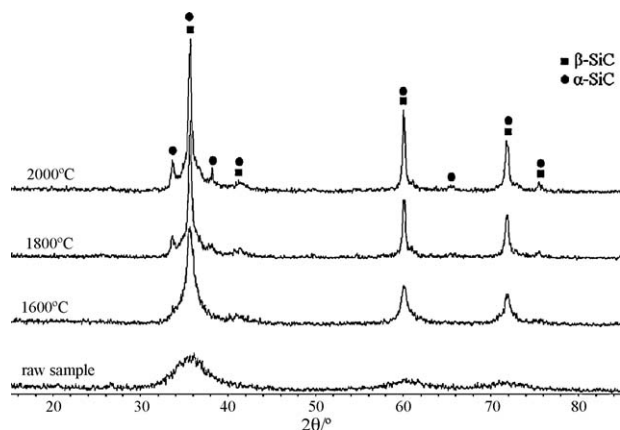


Fig. 4. Evolution of the XRD patterns recorded on the SiC ceramics with various temperature thermal treatments.

ceramics was annealed at 1800 °C,  $\alpha$ -SiC identified by two additional peaks at 34.08° ( $d = 2.628$  Å) and 38.15° ( $d = 2.357$  Å) was present [21]. Even after 2000 °C thermal treatment, there were both  $\beta$ -SiC and  $\alpha$ -SiC in the SiC ceramics, because the values of  $I_{34.08^\circ}/I_{35.65^\circ}$  and  $I_{38.15^\circ}/I_{35.65^\circ}$  were weak compared with the standardized XRD spectrum of  $\alpha$ -SiC.

In Fig. 3, the peaks located at 860 and 848  $\text{cm}^{-1}$  are called as the infrared-active ‘out of plane’ mode of the graphite. When the Raman inactive mode becomes Raman active by the modification of crystalline point group symmetry due to a slight rearrangement of lattice structure at the vicinity of the edge, the peak presence is possible [22].

Obviously, the shapes and positions of the peaks belonging to the modes of carbon in Fig. 5 are same as the Raman spectrum of turbostratically stacked particles [23]. And it was confirmed by the TEM image in Fig. 2(b).

Actually, the first-order modes (860, 1105, 1348, 1583 and 1625  $\text{cm}^{-1}$ ) of the turbostratic carbon in the Raman spectrum is also shown in Fig. 6, so the 1600 °C is deemed to the threshold of its formation, and the following reaction also happened [14]:

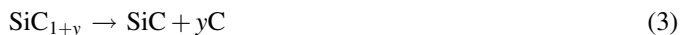


Fig. 7 shows TG curves of the SiC ceramics under air from 29 to 1200 °C. And the oxidation of free carbon phases introduced the weight loss of the SiC ceramics, and the weight increased by the oxidation of SiC phases. It is clear that the SiC ceramics with various temperature thermal treatments all began to lose weight near 600 °C. However, the biggest weight loss

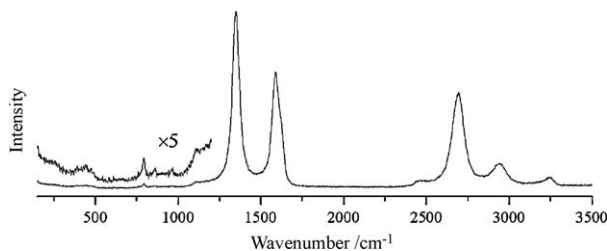


Fig. 5. The first- and second-order Raman spectrum of the SiC ceramics after 1800 °C annealing.

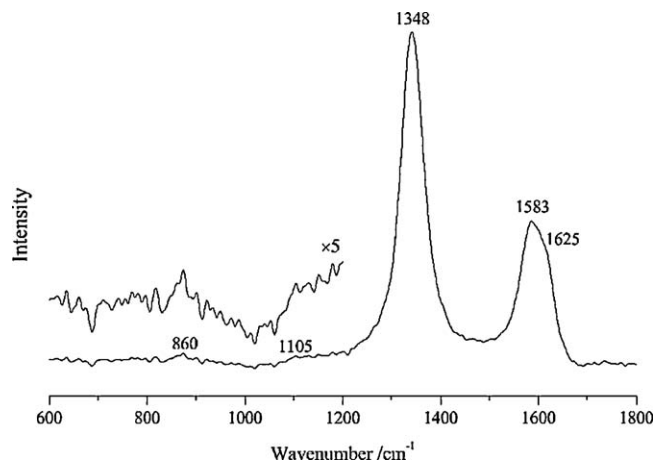


Fig. 6. The first-order Raman spectrum of the SiC ceramics after 1600 °C annealing.

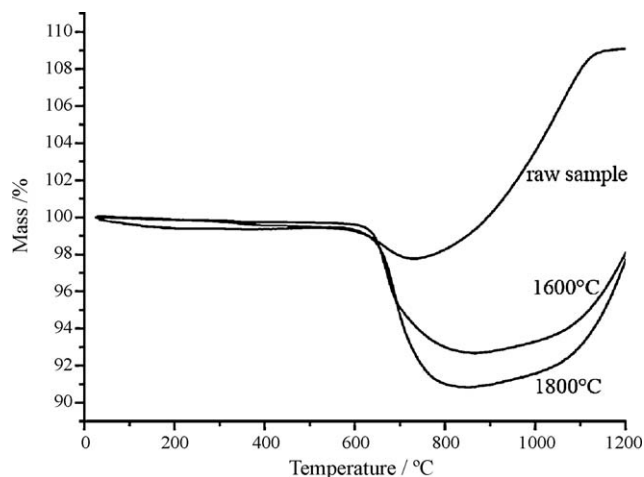


Fig. 7. TG curves of the SiC ceramics with various temperature thermal treatments.

ratio of the raw sample was 2.24 wt.% at 730.5 °C, while that of the SiC ceramics after 1800 °C annealing was 9.17 wt.% at 848.5 °C. And after 1600 °C annealing, the biggest weigh loss ratio of the SiC ceramics was 7.33 wt.% at 866.8 °C. Obviously, the oxidation behavior of the sample with 1600 °C annealing was similar to the sample with 1800 °C annealing due to the likeness of microstructures. So in the SiC ceramics with above 1600 °C annealing, the oxidation temperatures of the SiC phases were postponed more than 100 °C, because they were surrounded by the free carbon phases (seen in Fig. 2(b)).

#### 4. Conclusions

In conclusion, after high-temperature thermal treatments, Raman spectra were recorded for SiC ceramics derived from PCS. At the growth temperature 1200 °C, the amorphous SiC ceramics is formed and a part of the free carbon resolves in the SiC continuum as  $\text{Si}_{1-x}\text{C}_{1+x}$  phase. Then an ordering process of the SiC ceramics occurs after high-temperature thermal treatments from 1400 to 2000 °C. After 1800 °C thermal treatment, the SiC Raman fingerprints are present, while the



SiC crystallites have already been 7 nm surrounded by the turbostratic carbon. However, the 1600 °C is one critical point of the microstructure evolution from amorphous to turbostratic, because the  $I_D/I_G$  has the highest value after 1600 °C thermal treatment, and the first-order modes of the turbostratic carbon are present at the same time.

The oxidation behaviors of the SiC ceramics annealed at various temperatures are significantly affected by the microstructures of the free carbon phases. The biggest weight loss ratio of the raw sample is 2.24 wt.% at 730.5 °C, while that of the SiC ceramics after 1800 °C annealing is 9.17 wt.% at 848.5 °C. Due to the SiC phases surrounded by the free carbon phase, their oxidation temperatures are postponed more than 100 °C in the SiC ceramics with above 1600 °C annealing.

## Acknowledgements

The authors are grateful to National Natural Science Foundation of China (90916002) for financial support and Center of Material Science in the University of Defense Technology for Testing.

## References

- [1] S. Yajima, J. Hayashi, M. Otori, Continuous silicon carbide fiber of high tensile strength, *Chem. Lett.* 9 (1975) 1443–1477.
- [2] S. Matthews, M.J. Edirisinghe, M.J. Folkes, Effect of pre-pyrolysis heat treatment on the preparation of silicon carbide from a polycarbosilane precursor, *Ceram. Int.* 25 (1999) 49–60.
- [3] H.Q. Ly, R. Taylor, R. Day, Conversion of polycarbosilane (PCS) to SiC-based ceramic. Part II: pyrolysis and characterization, *J. Mater. Sci.* 36 (2001) 4045–4057.
- [4] A. Idesaki, Y. Miwa, Y. Katase, M. Narisawa, K. Okamura, M. Itoh, Ceramization process of polyvinylsilane as a precursor for SiC-based material, *J. Mater. Sci.* 38 (2003) 2591–2596.
- [5] N.I. Baklanava, V.N. Kulyukin, V.G. Kostrovsky, N.Z. Lyakhov, V.V. Terskikh, G.Y. Turkina, L.V. Zhilitskaya, O.G. Yarosh, M.G. Voronkov, High-temperature evolution of SiC/C products derived from preceramic polymers, *J. Mater. Synth. Process.* 7 (1999) 289–296.
- [6] L.V. Interrante, K. Moraes, Q. Liu, N. Lu, A. Puerta, L.G. Sneddon, Silicon-based ceramics from polymer precursors, *Pure Appl. Chem.* 74 (2002) 2111–2117.
- [7] S. Trassl, G. Motz, E. Rössler, G. Ziegler, Characterization of the free carbon phase in precursor-derived Si–C–N ceramics. Part I: spectroscopic methods, *J. Am. Ceram. Soc.* 85 (1) (2002) 237–244.
- [8] Y. Sasaki, Y. Nishina, M. Sato, K. Okamura, Raman study of SiC fibres made from polycarbosilane, *J. Mater. Sci.* 22 (1987) 443–448.
- [9] Z.F. Zhang, F. Babonneau, R.M. Laine, Y. Mu, J.F. Harrod, J.A. Rahn, Poly(methylsilane) – a high ceramic yield precursor to silicon carbide, *J. Am. Ceram. Soc.* 74 (3) (1991) 670–673.
- [10] R.M. Laine, F. Babonneau, K.Y. Blowhowiak, R.A. Kennish, J.A. Rahn, G.J. Exarhos, K. Wardner, The evolutionary process during pyrolytic transformation of poly(N-methylsilazane) from a preceramic polymer into an amorphous silicon nitride/carbon composite, *J. Am. Ceram. Soc.* 78 (1) (1995) 137–145.
- [11] A.C. Ferrari, J. Robertson, Interpretation of Raman spectra of disordered and amorphous carbon, *Phys. Rev. B* 61 (20) (2000) 14095–14107.
- [12] X.X. Jiang, R. Brydson, S.P. Appleyard, B. Rand, Characterization of the fibre–matrix interfacial structure in carbon fibre-reinforced polycarbosilane-derived SiC matrix composites using STEM/EELS, *J. Microsc.* 196 (1999) 203–212.
- [13] A.C. Ferrari, J. Robertson, Raman spectroscopy of amorphous, nanostructured, diamond-like carbon and nanodiamond, *Philos. Trans. R. Soc. Lond. A* 362 (2004) 2477–2512.
- [14] S. Karlin, Ph. Colomban, Raman study of the chemical and thermal degradation of as-received and sol–gel embedded Nicalon and Hi-Nicalon SiC fibers used in ceramic matrix composites, *J. Raman Spectrosc.* 28 (1997) 219–228.
- [15] F. Tuinstra, J.L. Koenig, Raman spectrum of graphite, *J. Chem. Phys.* 53 (1970) 1126–1130.
- [16] R. Vidano, D.B. Rischbach, New lines in the Raman spectra of carbons and graphite, *J. Am. Ceram. Soc.* 61 (1978) 13–17.
- [17] P. Kroll, Modeling the ‘free carbon’ phase in amorphous silicon oxycarbide, *J. Non-Cryst. Solids* 351 (2005) 1121–1126.
- [18] G. Gregori, H.J. Kleebe, H. Brequel, S. Enzo, G. Ziegler, Microstructure evolution of precursors-derived SiCN ceramics upon thermal treatment between 1000 and 1400 °C, *J. Non-Cryst. Solids* 351 (2005) 1393–1402.
- [19] S. Trassl, H.J. Kleebe, H. Strömer, Characterization of the free-carbon phase in Si–C–N ceramics: part II, comparison of different polysilazane precursor, *J. Am. Ceram. Soc.* 85 (5) (2002) 1268–1274.
- [20] H. Okumura, E. Sakuma, J.H. Lee, H. Mukaida, S. Misawa, K. Endo, S. Yoshida, Raman scattering of SiC: application to the identification of heteroepitaxy of SiC polytypes, *J. Appl. Phys.* 61 (1987) 1134–1136.
- [21] N. Janakiraman, M. Weinmann, J. Schuhmacher, K. Müller, J. Bill, F. Aldinger, P. Singh, Thermal stability, phase evolution, and crystallization in Si–B–C–N ceramics derived from a polyborosilazane precursor, *J. Am. Ceram. Soc.* 85 (7) (2002) 1807–1814.
- [22] Y. Kawashima, G. Katagiri, Observation of the out-of-plane mode in the Raman scattering from the graphite edge plane, *Phys. Rev. B* 59 (1999) 62–64.
- [23] P.H. Tan, S. Dimovski, Y. Gogotsi, Raman scattering of non-planar graphite: arched edges, polyhedral crystals, whiskers and cones, *Philos. Trans. R. Soc. Lond. A* 362 (2004) 2289–2310.